

## UHF Micromechanical Extensional Wine-Glass Mode Ring Resonators

Yuan Xie, Sheng-Shian Li, Yu-Wei Lin, Zeying Ren, and Clark T.-C. Nguyen

Center for Wireless Integrated Microsystems  
 Department of Electrical Engineering and Computer Science  
 University of Michigan, Ann Arbor, Michigan 48109-2122 USA  
 TEL: (734)647-1782, FAX: (734)647-1781, email: yxie@engin.umich.edu

### ABSTRACT

Vibrating polysilicon micromechanical ring resonators, utilizing a unique extensional wine-glass mode shape to achieve lower impedance than previous UHF resonators, have been demonstrated at frequencies as high as 1.2-GHz with a  $Q$  of 3,700, and 1.47-GHz (highest to date) with a  $Q$  of 2,300. The 1.2-GHz resonator exhibits a measured motional resistance of 560k $\Omega$  with a dc-bias voltage of 20V, which is 6X lower than measured on radial contour mode disk counterparts at the same frequency, and which can be driven down as low as 2k $\Omega$  when a dc-bias voltage of 100V and electrode-to-resonator gap spacing of 460Å are used. The above high  $Q$  and low impedance advantages, together with the multiple frequency, on-chip integration advantages afforded by electrostatically-transduced  $\mu$ mechanical resonators, make this device an attractive candidate for use in the front-end RF filtering and oscillator functions needed by wireless communication devices.

### I. INTRODUCTION

Having recently been demonstrated at frequencies past 1 GHz with  $Q$ 's  $>1,500$  in both vacuum and air [1], vibrating micromechanical (" $\mu$ mechanical") resonators are emerging as possible enablers for on-chip versions of the pre-select (or even channel-select) filters needed in the RF front-ends of wireless communication devices. The availability of such on-chip RF filters could greatly simplify the realization of future multi-band reconfigurable wireless communicators, which are expected to require many more RF filters than today's communicators—e.g., one set for each supported communication standard, as shown in Fig. 1. Unfortunately, however, although their  $Q$ 's and frequencies are now sufficient, the impedances of the GHz range  $\mu$ mechanical resonators demonstrated so far are still too high to allow direct coupling to antennas in RF systems, where matching to impedances in the range of 50 $\Omega$  and 330 $\Omega$  is often required.

As a solution to this problem, this paper presents a ring resonator structure with a unique extensional wine-glass mode shape capable of achieving higher frequency and lower impedance than previous UHF micromechanical resonators. This resonator operates in a special resonant mode, with a shape shown in Fig. 2(a), that combines aspects of two previously demonstrated modes, namely the extensional radial contour vibration mode [1][2] and the wine-glass disk vibration mode [3], together with the geometric advantages of a ring structure [4], to achieve the best of each design. In particular, this extensional wine-glass resonator design allows: (1) a high resonance frequency, owing to its use of an extensional mode; (2) a low motional impedance, due to its ring-geometry, which offers a larger capacitive transducer overlap area than provided by the

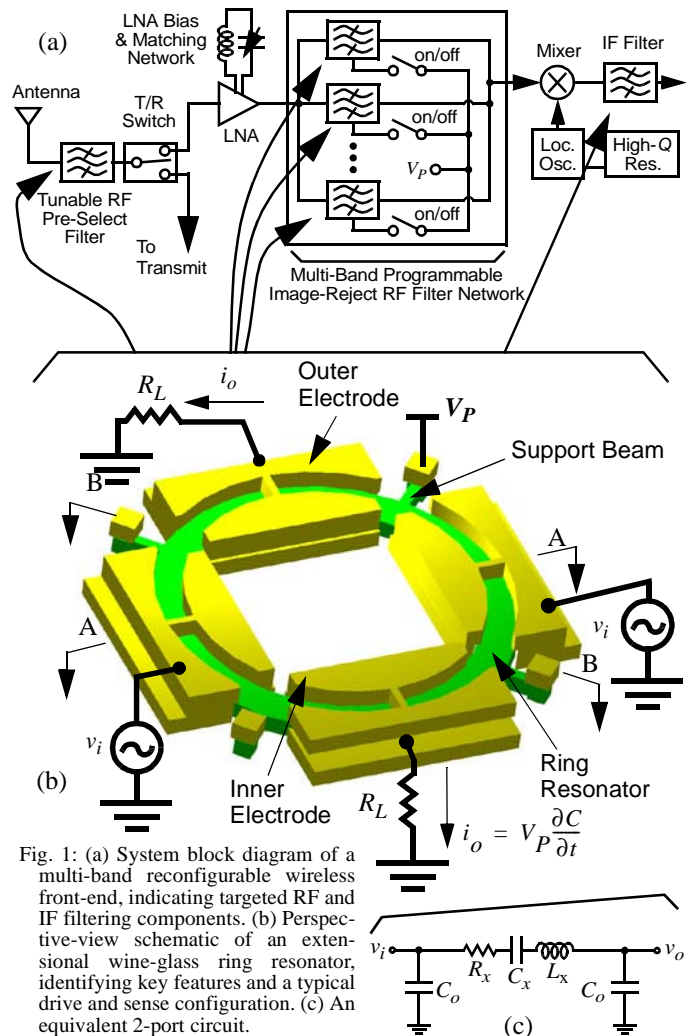


Fig. 1: (a) System block diagram of a multi-band reconfigurable wireless front-end, indicating targeted RF and IF filtering components. (b) Perspective-view schematic of an extensional wine-glass ring resonator, identifying key features and a typical drive and sense configuration. (c) An equivalent 2-port circuit.

perimeter of a filled disk; and (3) higher  $Q$ , since its mode shape resembles a wine-glass-like mode [3], which allows its support structure to avoid a centrally located stem and thereby reduce anchor losses. With this design, frequencies as high as 1.2-GHz with  $Q$ 's around 3,700, and at 1.47-GHz with a  $Q$  of 2,300, have been demonstrated, with motional resistances 6X lower than measured on radial contour mode disk counterparts.

### II. DEVICE STRUCTURE AND OPERATION

The key to attaining the higher  $Q$  of this resonator, relative to a previous solid disk counterpart [1], is in the support flexibility afforded by its extensional wine-glass mode shape, shown in Fig. 2(a). In this mode shape, the expansion (con-

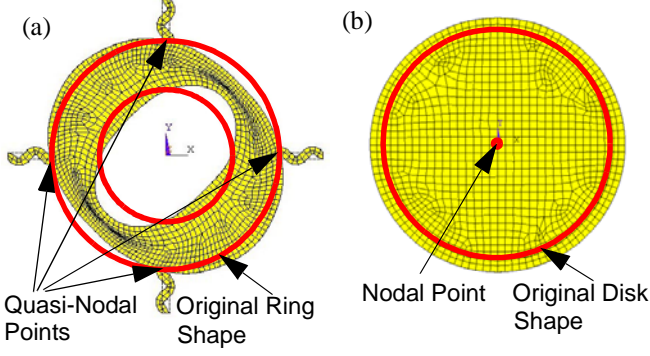


Fig. 2: Comparison of ANSYS-simulated resonance vibration mode shapes for (a) an extensional wine-glass mode ring resonator; and (b) a radial-contour mode solid-disk resonator.

traction) of the two diagonal quarters of the ring exhibit extensional characteristics, while the deformed inner and outer perimeters of the ring display wine-glass features. In contrast to the purely radial mode of a solid disk resonator, shown in Fig. 2(b), where the only nodal point is at the disk center, this extensional wine-glass mode offers several quasi-nodal points away from the center at which the ring may be supported. As demonstrated by previous (lower frequency) solid-disk wine-glass resonators [3], which achieved  $Q$ 's  $\sim 98,000$  at 73 MHz, the ability to support a disk resonator at its perimeter rather than its center can be advantageous for attaining high  $Q$ .

Fig. 1(b) presents the perspective-view schematic of the actual resonator design used in this work, identifying key features and an excitation configuration that instigates the extensional wine-glass mode of Fig. 2(a). As shown, this device consists of a ring suspended  $6,500\text{\AA}$  above the substrate by four tethers connected at nodal locations for this mode. The support beams are designed with geometries that isolate the resonator structure from its anchors in order to minimize energy losses to the substrate, allowing the structure to retain its highest  $Q$ . Aside from the support structure, multiple electrodes surround the ring, both inside and outside, to maximize the transducer overlap capacitance. To excite the device, a dc-bias voltage  $V_P$  is applied to the conductive ring and an ac voltage  $v_i$  to select drive electrodes. Together, these voltages generate an electrostatic force at the frequency of  $v_i$  that drives the device into resonance vibration when its frequency matches the resonance frequency  $f_o$ . Once vibrating, dc-biased (by  $V_P$ ) time-varying electrode-to-resonator capacitors generate currents that serve as the device output.

In effect, electrical input signals are converted to mechanical signals, processed (with high  $Q$ ) in the mechanical domain, then re-converted to electrical signals at the output, ready for further processing by subsequent transceiver stages. Electrically, this mechanical resonator device is equivalent to the  $LCR$  tank circuit shown in Fig. 1(c), and so is identical to that for any resonator, except with very high  $Q$ .

### III. DEVICE DESIGN AND MODELING

The dimensions needed to attain a specified resonance frequency  $f_o$  for an extensional wine-glass mode ring resonator can be obtained by solving the mode frequency equation [5]

Table 1: Ext. WG Resonator Design Possibilities

Parameter	$f_o=1.2\text{GHz}, Q=5,000$				
	85	22	85	85	50
$d_o$ [nm]	85	22	85	85	50
$t$ [ $\mu\text{m}$ ]	2	2	10	2	6
$R_{in}$ [ $\mu\text{m}$ ]	11.8	11.8	439.6	11.8	94.6
$R_{out}$ [ $\mu\text{m}$ ]	22.2	22.2	450	22.2	105
$P_{oe}$ [ $\mu\text{m}$ ]	70	70	1410	70	330
$V_P$ [V]	20	20	20	300	20
$R_x$ [k $\Omega$ ]	435	2	2	2	2

$$f_o = \frac{\alpha}{2\pi R_{out}} \sqrt{\frac{E}{\rho(1-\sigma^2)}} \quad (1)$$

where  $\rho$ ,  $\sigma$ , and  $E$  are the density, Poisson ratio, and Young's modulus, respectively, of the ring structural material, and  $\alpha$  is a parameter that depends upon the inner and outer ring radii,  $R_{in}$  and  $R_{out}$ , respectively, and on a matrix that specifies the mode shape. For  $R_{in}=11.8\mu\text{m}$  and  $R_{out}=22.2\mu\text{m}$ ,  $\alpha=20.35$  for the extensional wine-glass mode shape.

As with other vibrating resonators, the equivalent  $LCR$  circuit for the extensional wine-glass ring is governed by the total integrated kinetic energy in the resonator, by its mode shape, and by parameters associated with its transducer ports [6]. Using the procedure of [7], an approximate expression for the equivalent series motional resistance  $R_x$  of an extensional wine-glass ring resonator can be obtained. For an electrode configuration as in Fig. 4(b), with ports 1 and 2 used for input, and 3 and 4 for output, the  $R_x$  expression can be written as

$$R_x = \frac{\omega_o m_{re}}{Q V_P^2} \cdot \frac{d_o^4}{\epsilon_o^2 P_{oe}^2 t^2} \quad (2)$$

where  $P_{oe}=\pi R_{out}$ , and  $m_{re}$  is the equivalent mass of the resonator at a location opposite an electrode center, given by

$$m_{re} = \frac{\rho t \int_{R_{in}}^{R_{out}} \int_0^{2\pi} [U(r, \theta)]^2 r dr d\theta}{[U(r, \theta)]^2 \Big|_{r=R_{out}, \theta=0}} \quad (3)$$

where  $\omega_o$  is its radian resonance frequency, and  $U(r, \theta)$  is the mode shape. From (2), the best strategies for reducing  $R_x$  (in order of effectiveness) are to decrease the electrode-to-resonator gap spacing  $d_o$ , increase the electrode overlap perimeter  $P_{oe}$ , increase the device thickness  $t$ , and increase the dc-bias voltage  $V_P$ . Table 1 uses the 1.2-GHz design of this work to illustrate the effect that each of these parameters can have on the  $R_x$  of a given resonator design, and in the process, show just how small  $R_x$  can become with the right design. The table uses bold-faced print to indicate the variable/value that was altered to achieve an  $R_x$  of  $2\text{k}\Omega$ , which is small enough to allow on-chip  $L$ -network matching to an antenna. As shown in the last column, devices with  $2\text{k}\Omega$  impedance should be achievable with reasonably achievable geometric dimensions.

Due to its use of an extensional mode, the frequency of an extensional wine-glass resonator is determined primarily by the width of its ring, and not by its radius. Thus, the perimeter of the device can be made arbitrarily large to maximize its

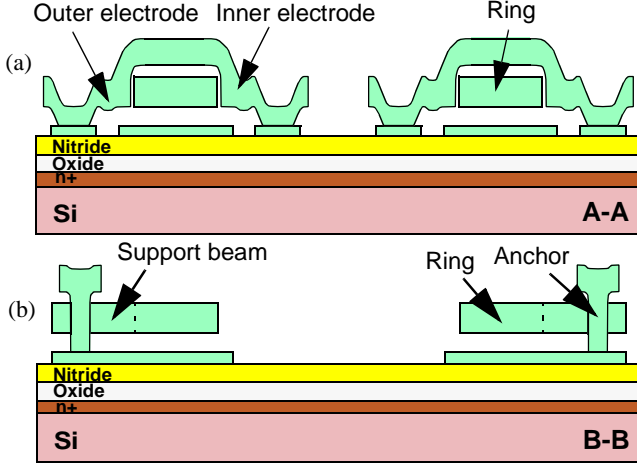


Fig. 3: Final device cross-sections. (a) Cross-section along AA' of Fig. 1(b) of a finished disk resonator, showing the overhanging polysilicon electrodes. (b) Cross-section along BB' of Fig. 1(b), showing the center and side supports after release.

transducer capacitance, hence, drive down its series motional resistance  $R_x$ . In addition, since the frequency of this device is determined primarily by its lateral dimensions, which are set by CAD layout, this device easily supports multiple frequencies on a single chip without the need for multiple film depositions. In contrast, counterparts with frequencies determined only by thickness (e.g., FBARs) require an additional film deposition for each additional frequency.

#### IV. EXPERIMENTAL RESULTS

Extensional wine-glass resonators with frequencies ranging from 400 MHz to 1.5 GHz were designed and fabricated using a process that combines polysilicon surface-micromachining with a sacrificial sidewall spacer technique to achieve  $\text{POCl}_3$ -doped polysilicon structures with polysilicon side electrodes, and with nano-scale electrode-to-resonator *lateral* gaps [1]. Figure 3 presents device cross-sections for an extensional wine-glass ring achieved via this process, taken through the lines indicated in Fig. 1(b). Fig. 4 presents SEM's (and dimensions) for 426-MHz and 651-MHz extensional wine-glass rings, as well as a zoom-in shot clearly showing the 85 nm lateral electrode-to-resonator gap achieved via the fabrication process.

The devices of Fig. 4(a) and (b) were tested under controlled pressures using a custom-built chamber with an electrical hook-up similar to Fig. 1(b), but using an RF input signal and local oscillator bias to suppress parasitic components via mixing [1]. No effort was made to impedance match devices to the measuring spectrum analyzer. This helped to preserve true  $Q$  values, but at the cost of *measurement* mismatch loss.

At first, only one set of electrode quarters (i.e., drive port 1, sense from port 3) were used. Fig. 5 (a) presents the frequency characteristic for the 426-MHz device of Fig. 4(a) measured under  $200\mu\text{Torr}$  vacuum, showing a  $Q$  of 7,700. Fig. 5(b) and (c) present measured spectra for the 651-MHz resonator of Fig. 4(b), showing very similar  $Q$ 's of 4,650 and 4,550 in vacuum and air, respectively, further demonstrating over the work of [1] that high stiffness, high frequency micromechanical resonators do not require vacuum to attain high  $Q$ . Fig. 5(d) presents the frequency spectrum of the 651-MHz device, measured

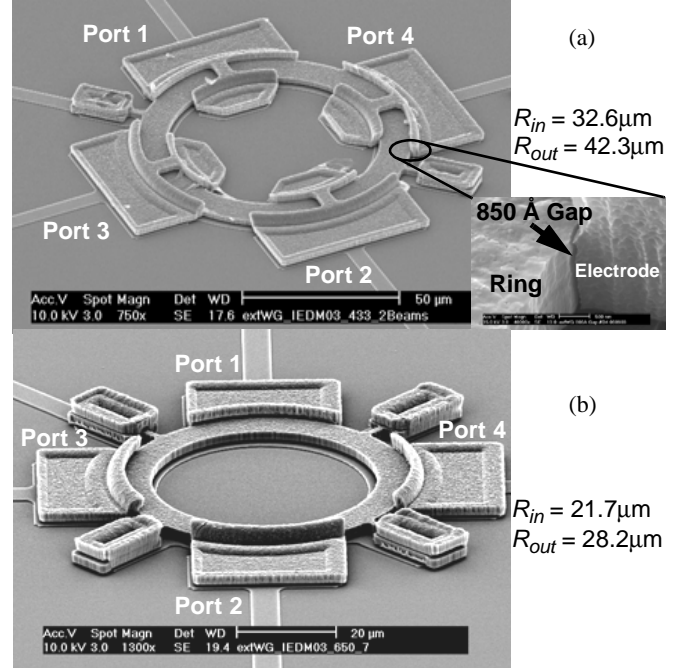


Fig. 4: SEMs of fabricated extensional wine-glass ring resonators. (a) 426-MHz device; (b) 651-MHz device.

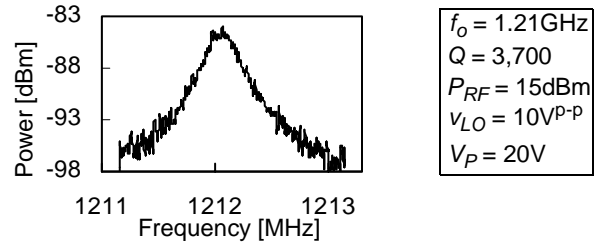


Fig. 6: Measured frequency spectrum for a 1.21-GHz, 4th-mode, extensional wine-glass resonator.

under vacuum, but this time using more electrodes: specifically, driving ports 1 and 2 and sensing via ports 3 and 4. Here, the additional ports provide a larger output, increasing the transmission power by more than 10 dB, and providing a smoother, noise-free spectrum. The motional resistance extracted from the data of Fig. 5(d) is  $\sim 280\text{k}\Omega$ , which is substantially lower than the  $4\text{M}\Omega$  previously measured for a 733-MHz disk resonator with a radius of  $10\mu\text{m}$  [1], proving the  $R_x$ -lowering ability of this design. If charge is placed on the ring structure to attain an effective dc-bias  $V_P$  of 100V, and the electrode-to-resonator gap spacing reduced to  $780\text{\AA}$ , (2) predicts an  $R_x$  of  $2\text{k}\Omega$ , which is in a range where an impedance match to an antenna can be achieved with an on-chip  $L$ -network.

By using higher extensional wine-glass modes, GHz frequencies can be achieved. Fig. 6 presents the frequency characteristic for a 1.2-GHz, 4th-mode, extensional wine-glass resonator measured in vacuum. The motional resistance extracted from the data of Fig. 6 is  $560\text{k}\Omega$ , which is 6X lower than the  $3.5\text{M}\Omega$  previously measured for a 1.14-GHz disk resonator with a radius of  $10\mu\text{m}$  [1], again showing the  $R_x$ -lowering ability of this design. Fig. 7 presents the measured spectrum for a 1.47-GHz, 4th-mode extensional wine-glass ring resonator in vacuum with a  $Q$  of 2,300. This represents

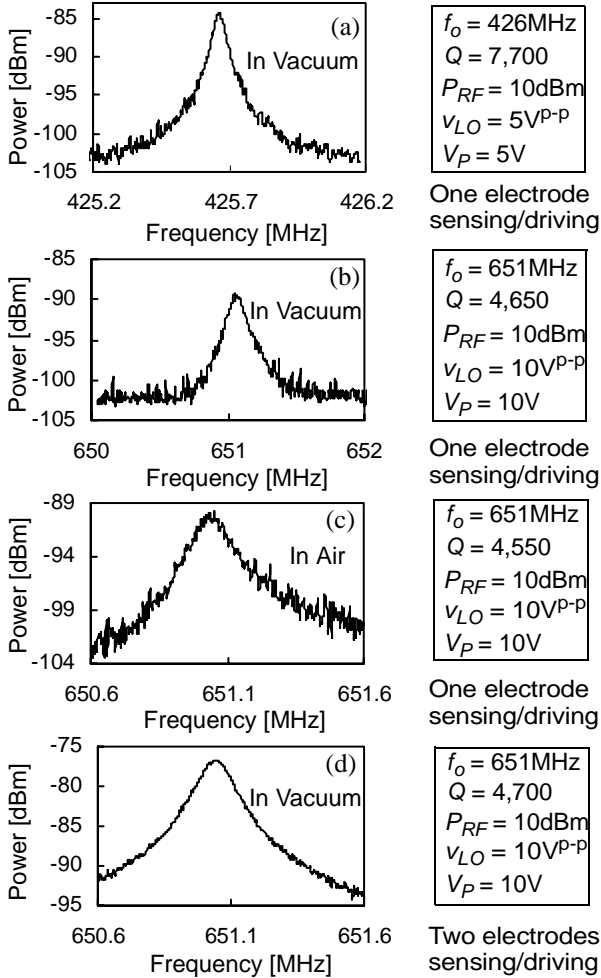


Fig. 5: Measured frequency characteristics for extensional wine-glass resonators. (a) 425.6-MHz resonator of Fig. 4(a); (b), (c), and (d) 651-MHz resonator of Fig. 4(b).

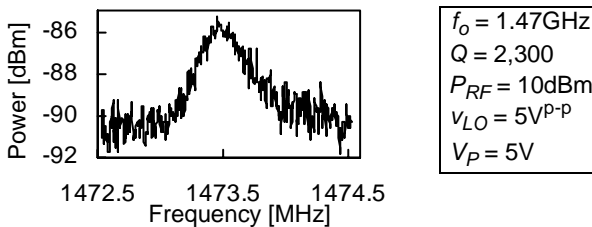


Fig. 7: Measured frequency spectrum for a 1.47-GHz, 4th-mode, extensional wine-glass ring resonator.

the highest frequency to date measured for polysilicon resonator devices. Table 2 summarizes each of the measured designs.

Finally, Fig. 8 presents a measured plot of fractional frequency change versus temperature for a 429-MHz extensional wine-glass resonator operated in its 2nd extensional mode. The uncompensated temperature coefficient of  $-11.2\text{ppm}/^\circ\text{C}$  is somewhat better than exhibited by previous polysilicon resonator designs [1][7]—yet another advantage of this design.

## V. CONCLUSIONS

The demonstration by this work of extensional wine-glass mode ring resonators with frequencies as high as 1.47-GHz,

Table 2: Ext. WG Resonator Design Summary

Parameter	Designed Frequency			
	425.3MHz	634.6MHz	1210MHz	1500MHz
$R_{in}$ [ $\mu\text{m}$ ]	32.6	21.7	11.8	33.7
$R_{out}$ [ $\mu\text{m}$ ]	42.3	28.2	22.2	42
Thickness [ $\mu\text{m}$ ]	2	2	2	2
Simu. $f_o$ [MHz]	426.8	638.9	1220	1528
Meas. $f_o$ [MHz]	425.7	651.0	1212	1473
$R_x$ @ $V_p=10\text{V}$	176k $\Omega$	280k $\Omega$	2.2M $\Omega$	200k $\Omega$
$R_x$ @ $V_p=100\text{V}$	1.76k $\Omega$	2.8k $\Omega$	22k $\Omega$	2k $\Omega$

$E = 150\text{ GPa}$ ,  $\rho = 2300\text{ kg/m}^3$ ,  $\nu = 0.226$ ,  $d_o = 85\text{ nm}$

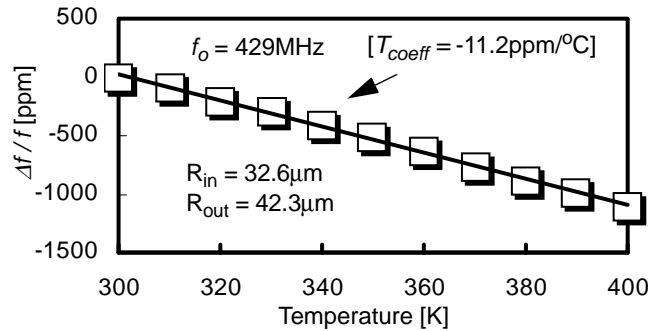


Fig. 8: Measured fractional frequency change versus temperature for a 2nd mode, 429-MHz extensional wine-glass ring resonator.

$Q$ 's  $>2,000$ , and impedances amenable to image-reject filtering and oscillator applications, should now put to rest any lingering doubts that micromechanical resonator technology can satisfy the RF frequency range needed by today's wireless communications. Although impedances low enough for direct connection with antennas were not demonstrated in this work, design paths based on the extensional wine-glass ring structure have been identified that should enable antenna-amenable impedances. In particular, substantially lower impedance is expected for designs that reduce electrode-to-resonator gap spacing, increase the structural film thickness, and increase the average ring radius, relative to those of the resonators demonstrated here. Research to further reduce impedance in this manner is underway.

**Acknowledgment:** This work was supported by DARPA Grant No. F30602-01-1-0573.

## References

- [1] J. Wang, Z. Ren, and C. T.-C. Nguyen, "Self-aligned 1.14-GHz vibrating radial-mode disk resonators," *Transducers'03*, pp. 947-950.
- [2] J. R. Clark, W.-T. Hsu, and C. T.-C. Nguyen, "High-Q VHF  $\mu$ mechanical contour-mode disk resonators," *IEDM'00*, pp. 399-402.
- [3] M. A. Abdelmoneum, M. U. Demirci, and C. T.-C. Nguyen, "Stemless wine-glass-mode disk  $\mu$ mech. resonators," *MEMS'03*, pp. 698-701.
- [4] B. Bircumshaw, G. Liu, H. Takeuchi, T.-J. King, R. Howe, O. O'Reilly A. Pisano, "The radial bulk annular resonator: towards a 50 $\Omega$  RF MEMS filter," *Transducers'03*, pp. 875-879.
- [5] G. Ambati, J. F. W. Bell, and J. C. K. Sharp, "In-plane vibrations of annular rings," *Journal of Sound and Vibration*, Vol. 47, no. 3, pp. 415-432, 1976.
- [6] R. A. Johnson, *Mechanical Filters in Electronics*. New York, NY: Wiley, 1983.
- [7] F. D. Bannon III, J. R. Clark, C. T.-C. Nguyen, "High- $Q$  HF microelectromechanical Filters," *IEEE J. Solid-State Circuits*, Vol. 35, no. 4, pp. 512-526, Apr. 2000.